

Design and construction overview for the Marathon Eagle aircraft

Wayne Bliesner
Boeing commercial Airplane Group
Renton, Washington

Abstract

An optimization study on the requirements to meet the challenge set forth by the Royal Aeronautical Society of flying a human powered aircraft a marathon distance in one hour is discussed. The Competition is the fourth event setup by the Royal Aeronautic Society under the sponsorship of Henry Kremer. The best achievements in human powered flight to date include:

- 1) The Daedalus project which flew 72 miles at 14 mph
- 2) The Muscular project which flew 1 mile at 30 mph

The Marathon Eagle project is the first attempt at flying 26 miles in one hour. Eleven previous human powered aircraft have been designed, built, and flown by the author. This new aircraft is the result of extensive design work in both 2-D and 3-D aerodynamic tailoring. The aircraft uses both high stiffness and high strength carbon fibre in the primary structure. It also uses moulded external surfaces with carbon and foam core construction similar to composite glider technology. The optimization work resulted in a fully cantilevered aircraft with an 85 foot span and an aspect ratio of 50.3. Improvements predicted in power levels required should allow flights on a regular basis with the record flight using a fit cyclist.

Induction

This report explains the design and construction interactions and decisions which took place to come up with the "Marathon Eagle" final configuration. This aircraft is targeted specifically to meet the Kremer Marathon competition rules as set out by the Royal Aeronautical Society. The report discusses the evolution of how the design came together with lessons learned from previous designs. Trade studies are presented showing the relative importance of each of the design variables. This produces a ranking of sub-design elements which need to be optimized and fed back into the overall optimization. Construction details and processes are examined and commented on. The final configuration is discussed along with current thoughts on how the airplane should handle in flight test.

Marathon Rules

The marathon course consists of five circuits around two pylons spaced 4051 meters apart with the start and finish line at the midpoint perpendicular to the

two pylons. The rules require a minimum altitude of 5 meters at the two pylons and crossing the midline on each circuit. The aircraft must accelerate under its own power during the start, which is being timed. The complete course consists of 5 circuits of the described closed loop. Two circuits are in one direction, the third is a figure eight, and the last two circuits are in the opposite direction. A successful landing is required to complete the requirements.

To efficiently fly this course minimum pylon turns are required as well as a rapid takeoff acceleration. For a typical human powered aircraft with a 300 foot turn radius the average speed required is approximately 26.2 m.p.h. depending on how close the pilot can hold to the course lines. For a turn radius of 600 feet this speed increases to 26.85 m.p.h.. For a 30 seconds delay at the beginning of the course, during the acceleration run, the average speed increases by .22 m.p.h..

Power Available by the Human Engine

Cycling performance has been measured extensively over the years due to the popularity of cycling activity and its use as a sport. A power verses time curve is shown in figure 1. The curve is plotted on a log scale to expand the region below 10 minutes. The human engine operates with a combination of two modes depending on the power intensity and duration. At the low time end power is generated anaerobically, without oxygen, and is limited by muscle size and the ability to withstand the high levels of lactic acid, which are generated during anaerobic exercise. This form of power is quite inefficient and lasts for only a few minutes. The second type of power is aerobic, with oxygen, this type of power is limited more by the bodies ability to process oxygen. The curve in figure 1 shows this high power level at the low time end and the lower power level at the higher time end. The last point on curve is at one hour, which is the maximum time available to complete the marathon course. The curve represents the power available for a first class athlete. This calibre of individual would be approximately a college athlete level but below an Olympic level. The value for one hour on this curve is .48 horsepower. Also included is a single point at 0.60 horsepower for one hour set by one of the best cyclist in the world, obtaining this calibre of individual for flight testing would be very difficult, however this does give a perspective as to the absolute limit of human power levels for one hour. The power levels

shown generally do not include the pilots weight, which is very important when it has to be lifted by the aircraft. Generally the power limits, shown in figure 1, are made by a fairly sizable athlete. The power level on this curve therefore needs to be factored by the pilots weight when considering the aircraft optimization task. If data is available on the pilots being considered this should be used for the aircraft optimization studies. For this study the author was used as a pilot/powerplant candidate as he had collected over 3 flight hours in human powered aircraft and has demonstrated a 0.48 sustained power level for 30 minutes, which is only slightly below the first class athlete line.

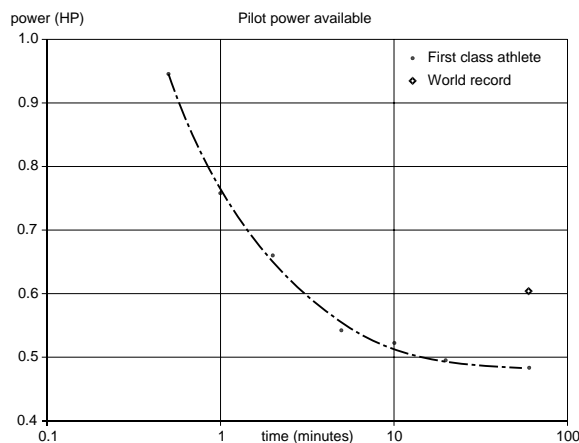


Figure 1. Maximum power output levels for the human engine from 30 seconds to one hour.

As the power required by the pilot is increased to near the maximum limit of the given athlete the ability to concentrate on controlling the aircraft decreases. The benefit is therefore quite large to obtain the best athlete available to obtain a large maximum power reserve or minimize the aircraft power requirements to be within the power levels of the available pilots. The ability to find the best combination of athletic ability and piloting skills is critical to the success of the project.

As a reference; the power level required by the Marathon Eagle is projected between .40 and .45 horsepower. The anticipated horsepower benefit, relative to previous designs, becomes quite important when the available group of athletic pilots is brought into the equation. The piloting precision effects how close the aircraft follows the minimum course distances. Deviations in the course add to the already high power levels making the task that much more difficult.

It should be noted that the power levels described in figure 1 are for person in a cycling position. This position has been optimized over the years to produce the maximum performance. Other cycling positions, which might be advantageous from an aircraft optimization perspective, are not as efficient especially in terms of maximum power available.

Aircraft History

As mentioned earlier a series of 11 human powered aircraft have been designed, built, and flown in the Seattle area by the author. The development of these aircraft started back in 1976 while studying for two Aeronautical engineering degrees at the University of Washington. The aircraft were built on an almost yearly schedule over 11 years. The goals at that time ranged from the figure eight course, to the English channel course, to a one mile speed course. The work tended to be done by a very small group of people which made it difficult to compete against the major groups involved at that time. Flights of over one mile including pylon turns were demonstrated with the later aircraft. A number of important lessons were learned which were directly applicable to the Marathon Aircraft. Some of the major points are listed:

- o A significant difference in maximum power available by the pilot was found between upright and recumbent piloting positions. For peak power levels the upright position was found to be more efficient. If the recumbent position was chosen training in that position was a necessity.
- o Propeller position and optimization was critical. Placing the thrust line as close to the vertical center of gravity as possible improved the handling characteristics of the aircraft. It was also found that putting the prop in front allowed it to operate in a clean flow-field and simplified the drive train which in turn reduced its losses.
- o Detail wing/fuselage tailoring is critical to the aircraft power level. The wing is operating in a highly loaded condition which makes it susceptible to drag increases if placed wrong on the fuselage. The spanloading tailoring across the fuselage is required to minimize the induced losses.
- o Aeroelastics must be included in the handling qualities of the aircraft. This may make the aircraft stiffness limited in the design cycle.
- o System reliability is important, especially for a small team, where design rebuilds and failures severely impact the success of the project.
- o Adequate pilot cooling and visibility must be included to reduce problems in flight test.
- o The ability to use brakes inside the aircraft is mandatory especially for small teams.
- o Excrescence drag is a very important item to track and minimize in the configuration
- o Ground handling points need to be considered to minimize wear during testing.

Preliminary Design

To optimize the configuration for the design requirements a series of perpetrations were analysed around the design point of 26.2 m.p.h.. Lessons learned from previous designs are incorporated as allowed. The general configuration is laid out to identify which areas of the design are more critical than others. This points

toward trends which require further aerodynamic or structural research to take full advantage of the optimization direction.

Figure 2 shows the overall configuration features for reference. The propeller is not included in the drawing.

The general configuration layout optimized with an upright pilot and the propeller in the front as low as possible. A conventional tail with an all moving horizontal and vertical were designed to include all internal linkages to minimize excrescence. High stiffness carbon was used in the bending fibres for the tail to minimize aeroelastic penalties. High strength carbon fibre was used elsewhere in the fuselage to minimize weight. The propeller optimized out at 9.5 foot diameter. This was sized from propeller efficiency and configuration integration trade studies. A driven-retractable landing gear was installed to minimize fuselage size and allow for a slightly larger propeller diameter which minimizes slipstream drag. The wing is integrated into the fuselage as a high wing configuration. The wing-fuselage region was extensively tailored to minimize superelevations at the junction and to maintain constant spanloading across the center section. The overall wing optimization and sizing issues are discussed next.

To carry out these trade studies as many of the features need to be modelled as possible. This allows the complete interactions to occur due to each perturbation. The wing sizing issues relate to the following areas:

- o Wing span
- o Wing area

- o Wing airfoil selection (or T/C interaction)
- o Ground effects

To study these interactions detailed buildup data is required for each variable. For airfoil characteristics the variations in: Reynolds number, drag polar shape, and thickness effects were included. Ground effect variations relative to span and height were also included. Detail weight buildups are included to obtain absolute speed envelopes and interactions with the sizing variables. The weight buildups of the primary and secondary structure were setup as a function of the span, wing area, and thickness.

Assumptions were made relative to semi-fixed items in the power equation. These include the following:

- o Propeller sizing and efficiency
- o Drive train efficiency
- o Structural design options
- o Fixed weights including pilot and fuselage
- o Stability and control characteristics
- o Overall excrescence levels

All of these variables are then combined into the aircraft power equations to obtain flight polars of the critical variables.

Figures 3 and 4 show wing size effects over the aircraft operating range. The average speed is estimated at 26.2 m.p.h. for this study. The minimum wing area is sized for the upper operational lift coefficient of 1.05 for the airfoil. The maximum lift coefficient for this study is 1.6. In these two figures the baseline is shown as the solid line with variations shown as dashed lines.

Figure 3 shows a large benefit with the span increase from 70 to 85 feet with a much smaller effect as span is increased further to 100 feet. This is an interesting trend when one considers the weight growth of 23 pounds which occurred in the wing when it was stretched from 70 to 100 foot

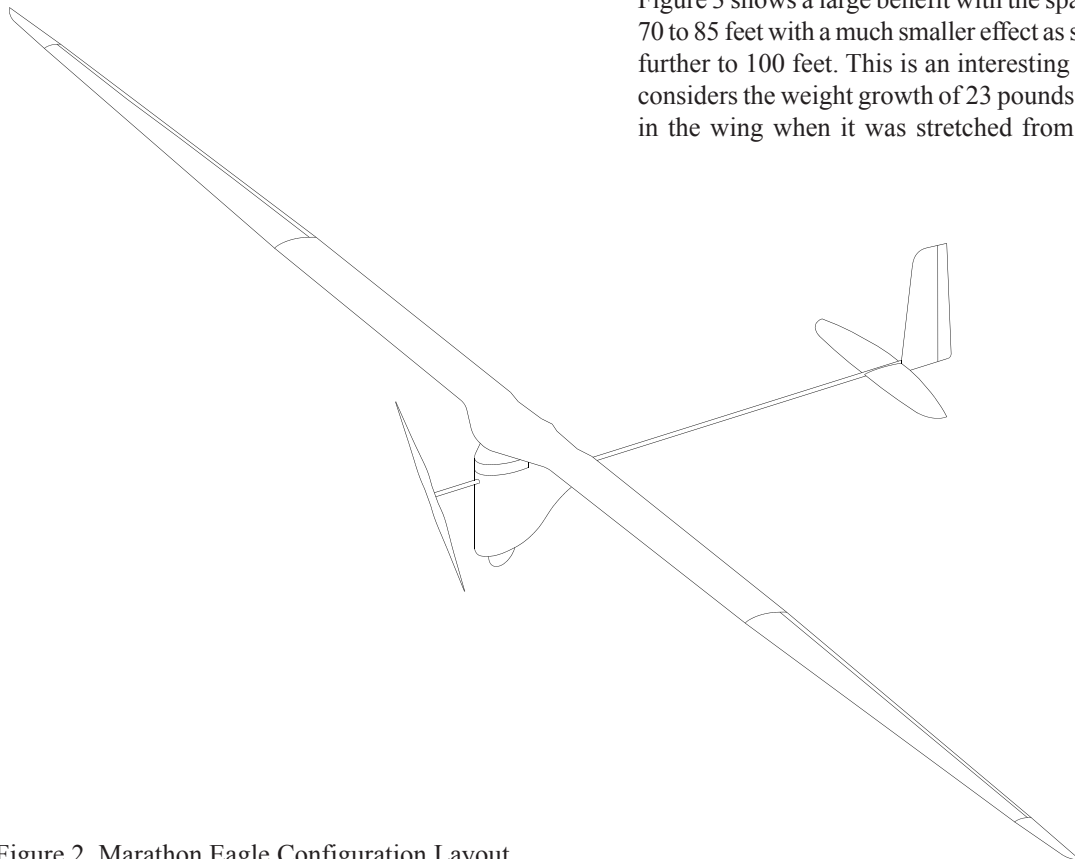


Figure 2. Marathon Eagle Configuration Layout

span, this represents a 33 percent increase in aircraft weight. For the initial span growth from 70 to 85 feet the induced drag effects are five times as large as the weight penalty effect.

An optimum dihedral for the high wing configuration was obtained from previous design lessons. The handling characteristics of the large spans were very poor with excessive dihedral even in mild wind conditions. Due to the very low roll rates a minimal amount of dihedral was found to handle the easiest. These wing configurations were stiffness limited, even with the use of a high modulus carbon fibre in the primary spar. This can be attributed to the very large aspect ratios and thin t/c , 11%, which the wing tended to be driven to for minimum power. The jig wing structure was built with anhedral in the center wing section so that spar weight could be reduced further while maintaining a maximum total 1-G dihedral.

The 85 foot limit was chosen to keep the outboard wing Reynolds number above 300,000. The wing airfoils have a sizable laminar bubble growth on the upper surface which occurs below this Reynolds number. The laminar bubble size causes a large non-linear drag increase to occur which must be dealt with using turbulation techniques. The span variations were designed at constant flying speed so that the chord dropped to hold area approximately constant. This lowered the outboard Reynolds number to around 250,000 on the 100 foot span case. The pylon turn further reduces the inboard wing tip Reynolds number. Both of these factors plus handling characteristics tend to

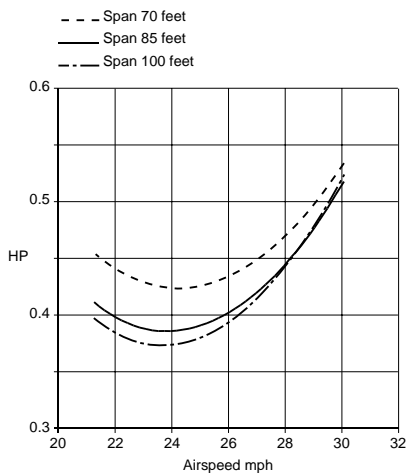


Figure 3. Effect of span variations around cruise design condition

favour the intermediate span case as a realistic optimum.

The wing area variation is shown in figure 4 for an 85 foot span and a wing t/c of 11%. The baseline area was determined from the cruise CL of 1.05. The second curve is a 10% increase in wing area which lowers the cruise CL. The increased wing area case has a 1.1 pound weight increase over the baseline. The small weight gain can be traced to the offsetting effects of the lower spar weight due to the absolute thickness increase of the larger wing chord. The second curve has a lower stall speed but has a .02 horsepower increase at the cruise speed. Due to these factors the smaller wing area was chosen. A second reason

for choosing the smaller wing area was that the baseline aircraft was sized for a 180 pound pilot which is towards to high end for pilot weights. A lighter pilot would optimize with an even smaller wing than the baseline.

It was found fairly early in the design study that the airfoil performance was very important in the total airplane performance levels. The FX-63137 was a 13.7% thick airfoil designed specifically for application in human powered aircraft designed back in 1963. This airfoil has a 60% laminar run on the upper and lower surface with care taken to minimize the laminar bubble penalties without special treatment to the wing. These airfoils were designed for the 300,000 to 700,000 Reynolds number regime. The large aft camber gave this airfoil a gentle stall progression at the expense of a sizable pitching moment. The pressure distribution at a Cl of 1.0 and drag polars for this airfoil are shown in figure 5. This figure also shows the pressure distribution for a 9.3% airfoil developed in 1990 by the author. This airfoil has a 100% laminar lower surface with a 70% laminar run on the upper surface. This resulted in the drag polars which are compared against the FX-63137 airfoil. The WT90093 airfoil uses a combination upper surface recovery with a more concave initial shape and a convex aft loading. The aft loading maintains the gradual stall characteristics. The drag polars show the significant reduction in drag at constant lift conditions over the total Reynolds number range.

Figure 6 shows a comparison of the WT90093 and a slightly thicker airfoil the WT91111. The second airfoil was designed for the outboard wing where the 15% chord aileron prevents the full lower surface laminar run designed into the thinner airfoil. The thicker airfoil, 11.1% t/c , has a lower surface transition location at 75% chord. The WT91111 has a slightly higher drag value relative to the 9.3% t/c airfoil but has a much more stable lower surface

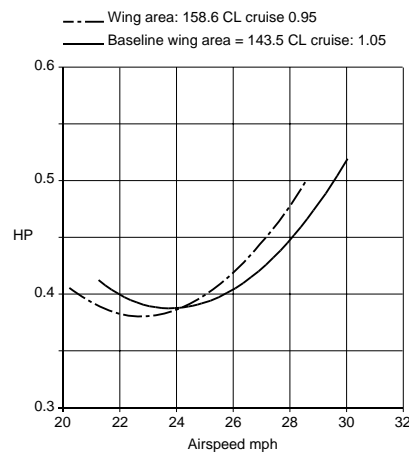


Figure 4. Effect of wing area variation relative to the minimum wing area baseline case

boundary layer. Studies with the full laminar airfoil showed the potential for the formation of Gortler vortices under certain conditions on the lower surface.

This would cause premature transition of the airfoil raising its drag level up to and possibly higher than the 11.1% airfoil. It was decided, based on this risk, to use the 11.1 percent thick airfoil as the baseline and to use the 9.3% thick airfoil only at the wing root where the transition location was not as critical due to the body intersection. The wing root junction benefited from the reduced superelevations and gradients generated by the thinner airfoil. The large pitching moment generated by these airfoils is a much smaller problem on this aircraft due the Marathon Eagles small wing chord and wing area. The use of a carbon wing skin is also beneficial in maintaining the correct twist distribution of the wing. The wing skin effectively doubles the torsional stiffness of the square tapered wing spars.

The importance of the wing airfoil optimization is shown in figure 7. The two airfoils, the 13.7% and the 11.1%, were compared in the total drag buildup package for the complete airplane. The two polars in figure 7 use an 85 foot wing span with the optimized wing area as described in figure 4. At the cruise condition of 26.2 mph the thinner airfoil combination has a 0.065 horsepower reduction relative to the 13.7 % thick wing. The 9.3% t/c airfoil showed a further reduction of .02 horsepower however, as mentioned earlier, the risk of using this airfoil was too high without a wind tunnel test to compare the two airfoils.

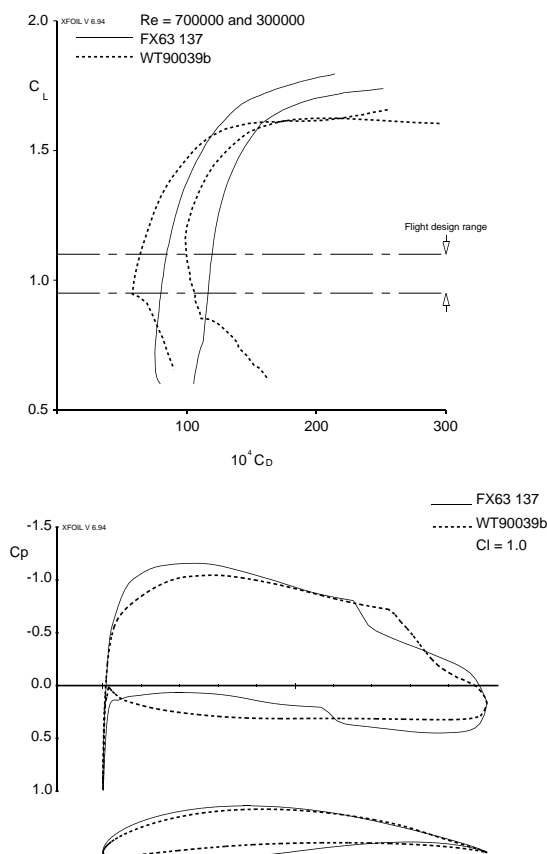


Figure 5. Pressure distribution and drag polar comparison

The use of airfoil t/c as a parameter, for airplane performance, was examined for a series of low Reynolds number airfoils with varying t/c and drag levels. The resulting comparisons produced an envelope of t/c vs drag which showed to have very little scatter at constant Reynolds number. By using values of drag on the envelope the “optimization” of a given airfoil can be established.

The next parameter relative to the airplane performance was ground effect. Theoretical drag reduction effects due to the reduction in trailing vortex strength are available. These curves show an increasing reduction in induced drag as the wing moves closer to the ground. A curve fit of this effect was included in the performance analysis for this design. Figure 8 shows the effect of flying at two altitudes, 17.4 feet and 10 feet. The height calculations were based on the lowest point on the airplane at cruise with the landing gear up. The height is adjusted up to the wing MAC height for the ground effect calculation. The 17.4 foot height is the 5 meter height mentioned in the marathon rules as the minimum height at 4 locations along each 5 mile leg, (one foot additional clearance was added to the 5 meters for flight tolerance). The 10 foot height was chosen as a possible intermediate height between the 4 markets to take advantage of the favourable ground effects. The curves show an increment of 0.04 horsepower for the lower altitude.

These comparisons were made using the 85 foot span configuration with the baseline wing area and the 11% thick wing. The beneficial effect of flying at lower altitudes, at first glance, appears to offer a definite advantage for the one hour course. This may not be the case however when one considers the flight around one circuit in its entirety. If we break the course into four sub-regions we have a requirement of 17.4 feet at each end of a 3 minute flight cycle. If we assume a 10 foot cruise height we will be operating at a lower power level over part of the 3 minutes however time is required to climb and descend for each cycle. The climb rate is a function of the extra power put out by the pilot, above the already high power level for cruise. For a 0.10 horsepower increase the time for the climb is approximately 40 seconds. If we assume a decent of 20 seconds then the lower altitude cruise lasts for 2 minutes per cycle.

In terms of total energy balance there is a net reduction in power required over the 3 minute cycle of 5 percent. This

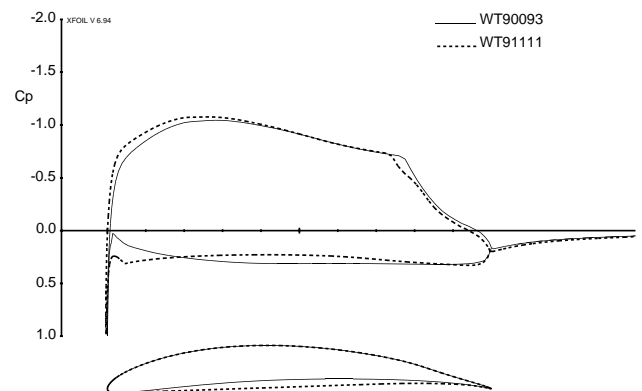


Figure 6. Comparison for the 9.3% and 11.1% t/c airfoils

is favourable as long as the pilot does not go into anaerobic power levels. The anaerobic power is taken out of the pilot similar to a battery storage with a very low efficiency level with approximately 17 times as much energy required to replace the anaerobic deficit after the workout with aerobic reserves. The amount of altitude change which is beneficial is very much a function of the pilots power reserves.

As a footnote to this problem it has been found that under certain conditions the power level for the aircraft actually increases at lower altitudes, Bryan Allen saw this when he was crossing the channel with wave action effecting the ground boundary layer. The theory which relates to this phenomenon involves the turbulent eddy size which is generated by wind conditions. These vary in size with ground height and are believed to be responsible for transitioning the wing boundary layer, which requires extensive amounts of laminar flow for minimum power. Thus under certain wind conditions the lower altitude may prove to be a disadvantage.

Wing-Fuselage Design

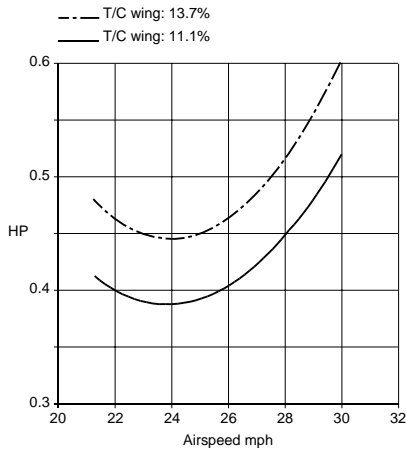


Figure 7. Wing thickness ratio effect on airplane performance.

The 3-D tailoring of the wing/fuselage junction is critical for a number of reasons. An estimate of ignoring this design region produces penalties of 0.05 horsepower and higher depending on the configuration chosen. A list of these issues are as follows:

- o The wing is fairly small and highly loaded relative to the fuselage. The large laminar runs, which are beneficial for these airfoils, can be forced to turbulent flow depending on the junction placement.
- o The high wing loading makes the wing upper surface boundary layer susceptible to turbulent separation by locally loading it further than the optimum.
- o The pilot should be recumbent for minimum aerodynamic interference however this does not lend itself to the optimum use of the pilots limited power level.

- o The upright fuselage has a lower aspect ratio than the recumbent fuselage making it more susceptible to sideslip losses.
- o The large fuselage relative to the small highly loaded wing results in a sizable local lift reduction on the wing which increases the induced drag of the total wing

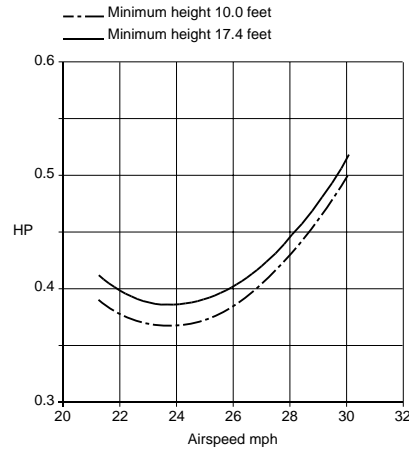


Figure 8. Airplane performance comparison at two minimum clearance altitudes due to ground effect

An optimization study into all of these variables resulted in the wing/fuselage configuration which is shown in figure 9. This figure shows a side view of the fuselage pod and wing center section. The internal primary fuselage structure is also shown. The tube extending off to the right goes back to the horizontal and vertical tail surfaces. The configuration incorporates a number of features to minimize the junction losses.

- o The wing is mounted above the fuselage, behind the attachment line on the leading edge. This maintains a laminar flow on the wing upper surface.
- o The wing chord size is increased on centerline to keep the wing loading constant across the junction.
- o The 9.3% airfoil is used locally to reduce the supervelocities and gradients in the junction region.
- o A retractable landing gear is used which allows a smaller fuselage in the lower fuselage region.
- o The landing gear is driven by the pedals to aid in the ground roll acceleration
- o The fuselage/wing structure is placed behind the pilot so as to not obstruct the pilots view
- o The air inlet is concentric around the propshaft to capture the turbulent airstream from the prop junction
- o The air from the inlet is blown up directly on the pilot and window to aid in cooling and maintaining a clear window
- o The propeller tip is below the fuselage to keep the prop tip vortex from impinging on the fuselage
- o The RPM of the prop is kept to a minimum so that the discrete turbulent wake sheets, generated by the prop, are reduced in frequency. The wake

- o packets traverse the fuselage once every 8.4 feet. Only one packet is on the fuselage at one time. Studies have shown that the flow changes back to laminar after the wake passes through.
- o The prop is moved as far in front of the fuselage as possible to minimize the distortion to the incoming prop face flowfield due to the fuselage
- o The back of the fuselage has a floating tab which acts to cancel the induced drag associated with sideslip manoeuvres.
- o The fuselage shell is made of a rigid composite construction to minimize fuselage width and distortion and to allow the highly contoured fuselage shape.
- o The fuselage shell is thinned from a 33% thick airfoil, in the middle of the fuselage, to an 8% thick airfoil at the wing junction.

Two fuselage airfoils were designed to operate at the cruise Reynolds number with minimum drag. The WT90026A airfoil has a more favorable pressure gradient and is used in the upper and lower extremes of the fuselage. The WT90026B airfoil is designed to allow additional clearance for pilots pedals and controls over the middle of the fuselage. The two airfoils are shown in figure 10 at zero degrees sideslip.

The two airfoils shown in figure 10 were analysed at 26 percent thickness the fuselage was actually built with 33% thick airfoils. The reason for the discrepancy is due to the 3-D nature of the pressure field generated by the fuselage/wing combination. The minimum pressures on the fuselage side, at zero sideslip, act like 2-D pressures on a 26% thick airfoil. A 3-D contour plot is shown in figure 11. The figure shows the side view of the fuselage with pressure coefficient contours superimposed on the shape. The contours are shown for every 0.20 delta Cp from +1.0 at stagnation to -0.60 at the minimum region.

The pressure distribution shows the favorable gradient over the majority of the middle of the fuselage. This should allow a sizable run of laminar flow to occur between propeller blade passages. The pressure also show the reduced pressures on both the lower and upper body regions. The lower body region recovery occurs farther forward where transition is likely to occur earlier due to the local 3-D flowfield. The Cp's at the fuselage/wing junction are considerably lower than the center of the fuselage indicating the benefit of the wing/fuselage optimization.

Figure 12 shows the 3-D wing upper and lower surface pressure coefficient contours at the cruise condition. The upper surface pressure contours are seen to be fairly uniform across the junction. The leading edge sweep was kept small enough so as not to produce a turbulent attachment line due to crossflow instabilities. The lower surface pressures shows the increase in the local velocities relative to the wing region away from the junction. The 9.3% thick airfoil is blended into the 11.1% thick airfoil outside of the blending region.

Figure 13 shows the WT90026B 2-D airfoil at a sideslip angle of 4 degrees. The flap is deflected at an

angle of -6.0 degrees to produce a zero loading condition. A boundary layer analysis at this condition shows fully attached flow.

Figure 14 shows the 3-D analysis for a 10 degree sideslip with the flap at -6 degrees. The pressure coefficients are shown on both the upper and lower surfaces. The pressures in the 2-D case match the 3-D levels as closely for the sideslip case as they did for the cruise case.

For the 10 degree sideslip case without the fuselage flap the induced drag, from the fuselage, increases by 0.12 horsepower. The benefit from the fuselage flap becomes quite effective in allowing the fuselage to fly at small sideslip angles with little or no penalty.

Propeller Design

The propeller design utilizes the code developed at MIT which accounts for both axial and circumferential induced flowfield effects on the optimization. The propeller is designed to produce as high an efficiency as possible at cruise while allowing good performance for climb capability at maximum power. The prop was designed to maintain a minimum Reynolds number of 100,000 to minimize parasite drag effects. This resulted in a 9.5 foot diameter prop spinning at 2.3 revolutions per second. The prop airfoil was the E193 which operated at

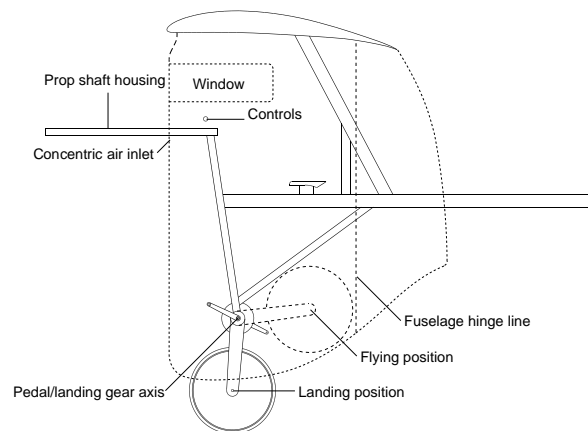


Figure 9. Fuselage layout

a cruise lift coefficient of 0.60 at 0.40 horsepower. The efficiency at cruise was estimated at 91%.

The lower graph in figure 15 shows the spanloading curves at cruise and max climb out power. The upper graph shows power verses efficiency at the cruise speed of 26.2 mph. The curve shows the high efficiency maintained over the complete horsepower regime from 0.40 to 0.80. The dot at 0.40 hp is for the prop with natural transition on the airfoil. The curve assumes pneumatic turbulators at 0.50% chord on the prop upper surface.

Figure 16 shows the efficiency curves used to make

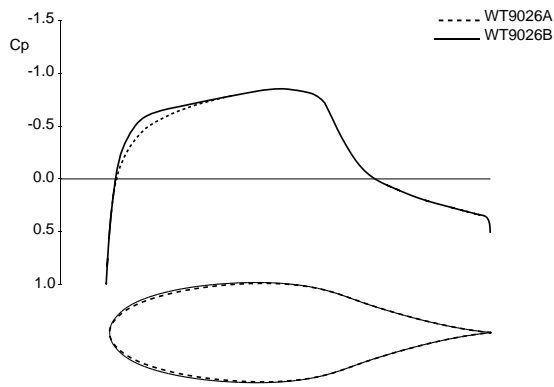


Figure 10. 2-D analysis of fuselage airfoils

the propeller design choices. Both curves are at the cruise speed and power levels. The top curve shows the effect of radius. Four and three quarters foot radius was chosen based on maximizing diameter for efficiency reasons and minimizing the gear length, thrust line, and cruise altitude requirements (with the gear retracted the prop is the lowest item going over the height bar). The second curve shows the effect of prop rotation speed on efficiency. The value of 2.3 RPS was chosen to minimize the effects on the fuselage by the propellers wake.

The propeller operates most efficiently at the cruise speed. At lower speeds the maximum power available drops rapidly. To get around this problem the drive wheel is equipped with a spring loaded release pin. This pin is manually engaged prior to takeoff and is held in place as long as torque is being applied from the pedals to the wheels. Figure 17 shows the propeller behaviour as the

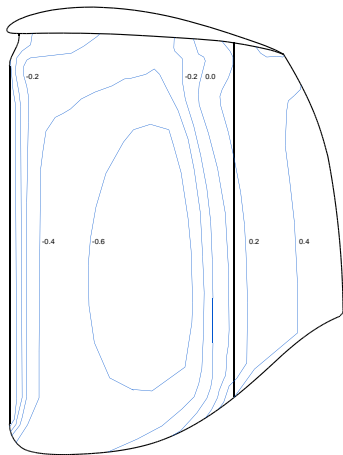


Figure 11. Pressure coefficient contours on the fuselage at cruise conditions

airplane is accelerating to takeoff. The top solid line shows the maximum power which the propeller can produce as a function of speed. The dashed line shows the actual power absorbed by the propeller when it is pinned to the wheel speed. For a takeoff power of 0.60 hp you can see that the wheel is absorbing the majority of the loading up to takeoff. By momentarily dropping the power the pin disengages and the propeller takes over up through takeoff. The disengagable pin technique has the further advantage

on landing in that snatch loads do not occur in the propeller drive system.

Wing Spar Construction

The optimization process for the aircraft wings required that the spars be investigated to determine if improvements could be made relative to round spars. These are manufactured by using a prepreg carbon wrapped in a helix of + and - 45 degree layers for torsional stiffness and 0 degree caps to carry bending load. The round spars place the cap at a varying offset relative to the spar axis which is a penalty. Using a square spar allows constant fibre stress on the bending cap fibres. By tapering the spar, across the span, the maximum spar thickness can be achieved everywhere along the wing thus maintaining the lowest weight for a given thickness. The process for constructing the spar was as follows:

- o Mill a .25 inch radius square 1/8 in. thick tubing.

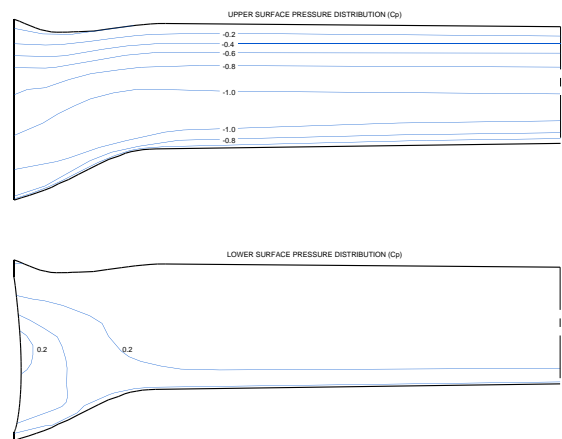


Figure 12. Upper and lower surface pressure contours at the wing junction due to the combined wing/fuselage interference and tailoring

- o Taper one tube to match the outboard thickness and reglue with 500 degree epoxy.
- o Sand both mandrills to 600 grit smoothness.

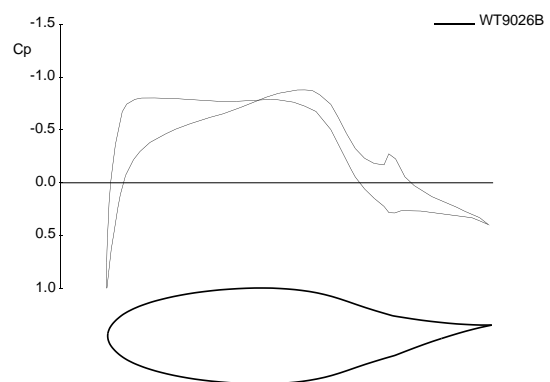


Figure 13. 2-D analysis of the middle fuselage airfoil at an equivalent 3-D sideslip angle of 10 degrees

- o Coat the mandrills with Teflon to allow part release
- o Build torsional clamping fixtures to hold mandrills during 350 degree F cure cycle (square mandrills will warp when heated)
- o For wing center mandrill build a clamping fixture

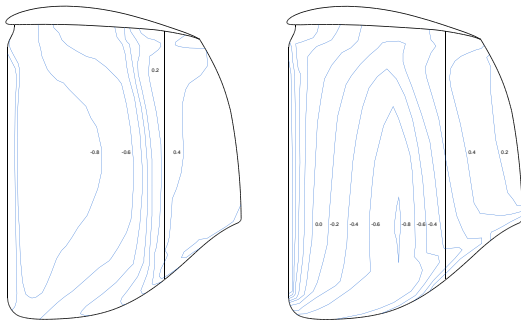


Figure 14. 3-D fuselage pressure coefficient contours for a 10 degree sideslip with the fuselage flap at -6 degrees

- o to obtain a negative curve for wing anhedral
- o Spars are laid up using a T-300 carbon for the torsion and compression caps. P-75 carbon is used for the tensile cap.
- o The tapered mandrills are slid out of the parts after curing, the square tube required chemical milling to remove the mandrill

Wing Skin Construction

A carbon sandwich construction was chosen on all external surfaces of the aircraft. This was done to minimize excrescence problems found with the mylar skin techniques. It also allowed closer 3-D curvature matching of the final airplane shape. To keep the skin weight as low as possible a 0.50 oz/sq yard carbon mat was found which could be laid up on either side of a foam core. This technique produced an extremely rigid and strong skin with a weight of .08 pounds per square foot. The performance trades on the airplane indicated that the improvements in drag due to the better surface finish outweighed the weight penalty for the skin. The skin also acts as a torsional member for the parts, however all components are designed to carry full torsional load in case of skin failure. Detail moulds had to be created of all parts. The moulds were split into an upper and lower half with an alignment flange on the moulds to allow for accurate final assembly. The parts are made by applying a colored epoxy coating inside the molds over the wax surface, this becomes the outer part surface. The carbon is squeegeed to an 80% glue ratio and applied to the molds. Earlier plans were to reduce this glue ratio however the thin weave would not allow a structural part with glue ratios below 80%. The carbon and foam are held in place under a vacuum until cured. The enormity of this task was not realized until after it was too far along to change. The technique described above will work, several parts have already been built, however the improvements in mylar construction techniques may have allowed a faster alternative.

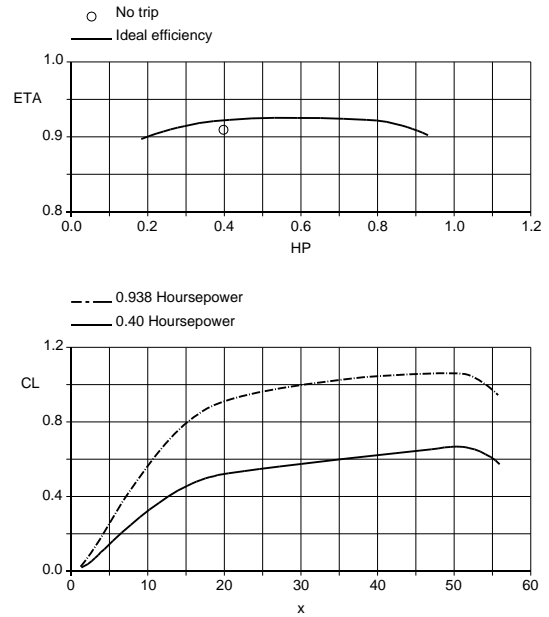


Figure 15. Propeller efficiency versus power and spanloading for the optimized configuration

Controls and Handling Characteristics

This airplane uses full 3-axis controls mounted on the control column which also serves as the handle bars. The elevator is controlled by a twist grip in the right hand, the rudder by moving the bar left and right, and the ailerons by rocking the bar from side to side. The wheel brake is located on the left handlebar. The wheel retract handle is located on the left side just below the controls, a protective fairing covers the drive chain so that the retract handle can be reached without touching the chain. The airplane uses an all flying horizontal and vertical. High aspect ratio ailerons are used on the outboard wing panels. All of the controls use internal gearing at the control surfaces.

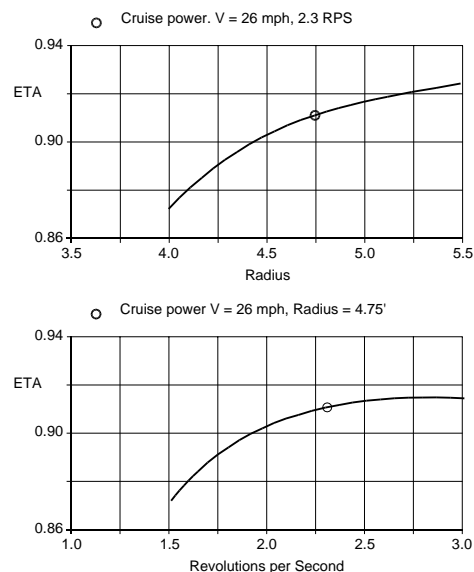


Figure 16. Propeller optimization curves at conditions

The handling characteristics were setup similar to the last versions of airplanes tested by the author. The thrust line is as low as possible to minimize the pitch due to thrust change effects which can be quite large. The pitch axes has a sizable static stability margin. These aircraft exhibit a low frequency pitch mode which is very difficult to damp and control. The increased pitch stability improves this problem. Having a large static stability in pitch is beneficial as these airplanes tend to fly at one design point for minimum power. The rudder is used more than the aileron for turning and course corrections. The ailerons cause a large adverse yaw when used and make it difficult for small corrections. The rudder is much more ideal for control as it produces a direct coupling of the yaw with the rudder angle. The roll rate is very slow with the rudder

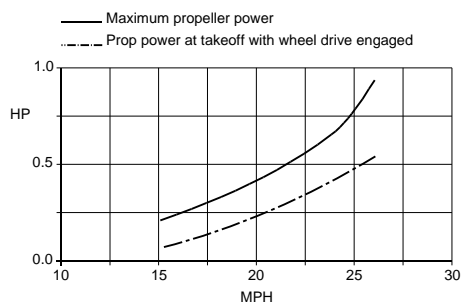


Figure 17. Drive power during takeoff roll on propeller on 2-24 ft lengths of wing

and is in the same direction as the yaw. For turning the rudder is used to initiate the roll and opposite ailerons are used to hold the adverse roll effect due to the large dynamic pressure variation across the wing which occurs at the typical turn radiuses. The large span is always a handling problem, especially in winds, however the very high aspect ratio allows a faster roll rate making the aircraft easier to control.

It is expected that some tuning of the aerodynamics will occur during initial testing. Plans include using pneumatic turbulators on the wing and propeller once transition locations are verified. Power available should be within the capability for obtaining initial flights of several minutes which will allow a rapid learning curve for this aircraft. As this is a completely new design with completely new hardware relative to previous designs there will probably be a few unforeseen problems. The large database collected with previous aircraft was very beneficial in minimizing this effect.

Notes. This paper is reproduced from:

Bliesner, Wayne. Design and construction overview for the Marathon Eagle aircraft. in AIAA International Human-Powered Flight Symposium. Seattle Washington 1994.

and:

Bliesner, Wayne. The Design and Construction Details of the Marathon Eagle. "Technology for Human Powered Aircraft." Proceedings of the Human-powered Aircraft Group Half Day Conference. The Royal Aeronautical Society, London, 30 January 1991.

I redrew all the figures to improve readability compared with scanned images. Where Wayne's airfoil data was calculated using Boeing codes I had used XFOIL as a check of Wayne's calculations when he was designing the aircraft and I have used these for figures 5 and 6 here. All other figures are tracings of Wayne's plots. I replaced figure 2, which showed the marathon eagle panel mesh used for design with a drawing showing the aircraft configuration. The vertical stabiliser was replaced during testing after both these papers were published and this is shown in the new drawing.

J McIntyre June 2003